Ab initio study of native defects in SiC nanotubes

R. J. Baierle* and P. Piquini
Departamento de Física, Universidade Federal de Santa Maria, 97105-900, Santa Maria, RS, Brazil

L. P. Neves
Centro Universitario Franciscano, Rua dos Andradas 1614, 97010-032, Santa Maria, RS, Brazil

R. H. Miwa
Instituto de Fisica, Universidade Federal de Uberlândia, Caixa Postal 593, CEP 38400-902, Uberlândia, MG, Brazil
(Received 22 December 2005; revised manuscript received 18 July 2006; published 23 October 2006)

Spin-polarized density functional theory is used to investigate the electronic and structural properties of vacancies and antisites in zigzag, armchair, and chiral SiC nanotubes. Antisites present lower formation energies compared to vacancies, introducing an empty electronic level close to the bottom of the conduction band for both cases Si_C and C_{Si}. A carbon vacancy introduces a pair of electronic levels (bonding and antibonding) within the band gap. A silicon vacancy presents the highest formation energy and introduces one occupied level (spin up) resonant within the valence band and three nearly degenerate spin-polarized levels, one for spin up and two for spin down, within the nanotube band gap.

DOI: 10.1103/PhysRevB.74.155425 PACS number(s): 73.20.At, 71.15.Nc, 73.22.−f

I. INTRODUCTION

Carbon nanotubes (CNTs) were identified for the first time by Iijima in 1991 as by-products of arc discharge experiments.[1] They are light and flexible, have a high elastic modulus ($\approx$1 TPa), and show electronic properties that are dependent on their diameters and chiralities.[2–4] These unusual features allow one to consider CNTs as candidates for several applications in "nanoengineering" as well as leading to the discovery of new physical properties in quasi-one-dimensional structures. The successes in synthesizing CNTs prompted experimental and theoretical efforts on nanostructures of other elements. For instance, tubular structures of III-V compounds have been theoretically predicted[5,6] and experimentally synthesized,[7–10] with promising applications being envisioned in many different areas.[2] Silicon nanostructures, specially silicon nanowires,[11] are now the focus of intense research. Theoretical studies, based on *ab initio* total energy calculations, proposed the formation of stable phases of silicon nanotubes,[12,13] but no stable forms have yet been experimentally obtained.

Very recently, silicon carbide (SiC) nanostructures like nanorods, nanowires, and nanocables have been verified by numerous experimental works.[14–17] Meanwhile, theoretical investigations addressing the stability of SiC nanostructures have been performed, based on *ab initio* total energy calculations. Wang *et al.*,[18] using density functional theory (DFT) with the B3LYP functional, studied the structure and stability of cagelike $(SiC)_n$ (n=6–36) clusters, suggesting an energetically stable $(SiC)_{12}$ cluster structure. The interest in SiC nanostructures derives primarily from their exceptional properties such as thermal stability, chemical inertness, high thermal conductivity, high reactivity of the external (internal) surface, and others,[19,20] which make them candidates for nanodevices that operate in harsh environments.[21] Very recently silicon carbide nanotubes (SiCNTs) have been successfully synthesized,[22–26] opening up a new class of nanotube structures. However, different from CNTs, III-V BN nanotubes, and the carbon-BN mixed nanotubes, there are few theoretical studies addressing electronic and structural properties of SiCNTs. Mavrandonakis *et al.*,[27] using DFT in the cluster approach, argued that SiCNTs should not maintain the tubular form for Si to C ratios greater than 1, with Si-rich tubes preferring to arrange as nanowires or clusters. On the other hand, calculations using periodic boundary conditions and large unit cell approaches[28–30] show that SiCNTs are stable, with greater stability predicted for the tubes with alternating Si-C bonds. These calculations also show that SiCNTs are always semiconducting. The energy band gap of SiCNTs is weakly dependent on their chirality (in contrast to CNTs), with direct band gaps for zigzag tubes $(n,0)$ and indirect gaps for armchair and chiral tubes.

Since SiCNTs are grown far from thermodynamic equilibrium, viz., SiCNTs can be produced by SiO reaction with CNTs at about 1200 °C,[23] the formation of numerous native defects is expected. Thus, the characterization of such defects is quite important not only for basic research on one-dimensional (1D) (or quasi-1D) nanostructures, but also for future technological applications of SiCNTs in nanodevices. In this work, following previous theoretical studies,[27–31] we have studied the native defects in SiCNTs. Through *ab initio* total energy calculations, within the density functional theory, we determined the formation energies, equilibrium geometries, and electronic properties of antisites and vacancies in SiCNTs.

II. METHODOLOGY

The calculations are based on first-principles density functional theory, using the local spin density approximation (LSDA) for the exchange-correlation term,[32] as proposed by Perdew-Zunger.[33] We have used the SIESTA code,[34] which self-consistently solves the standard Kohn-Sham (KS) equations. The KS orbitals are represented by linear combinations

of numerical pseudoatomic orbitals (PAOs), similar to the ones proposed by Sankey and Niklewski.[35] In all calculations we used a split-valence double-ζ quality basis set, enhanced by a polarization function, as provided by the SIESTA code. In order to define the confining radii of the original (first-ζ) PAOs for all the species (C and Si), an energy shift of 0.25 eV was used. To project the charge density in real space and to calculate the self-consistent Hamiltonian matrix elements a cutoff of 80 Ry for the grid integration was utilized. The interaction between the ionic cores and the valence electrons is modulated by nonlocal *ab initio* norm-conserving pseudopotentials.[36,37] The Brillouin zone was sampled by $(1\times1\times5)$ mesh points in the **k** space within the Monkhorst-Pack scheme,[38] resulting in three special **k** points along the tube axis. In the self-consistent procedure, the occupation of the electronic states near the Fermi energy is smeared by attributing an electronic temperature to the system. The electronic levels are occupied according to the Fermi-Dirac distribution. This procedure is generally used to increase the rate of convergence of the self-consistent cycles. An electronic temperature of 50 meV has been used for most of the calculations. In the special case of V_{Si}, the electronic temperature was set to zero in order to circumvent a possible reordering among the levels in the gap, as discussed in Sec. III B.

Our study is performed using three tubes with different chiralities: a (10,0) zigzag tube with a 9.924 Å diameter, a (6,6) armchair tube with a 10.312 Å diameter, and an (8,4) mixed tube with a 10.534 Å diameter. We use periodic boundary conditions and a tetragonal supercell with a lattice constant of 18 Å in the directions perpendicular to the tube axis. The supercells for the (10,0), (6,6), and (8,4) SiCNTs have three 120-atom, four 96-atom, and one 112-atom unit cells along the tube axis, respectively. All the atoms in the enlarged unit cells are relaxed. The forces are calculated using the Hellmann-Feynman procedure and the geometries are optimized using the conjugated gradient scheme. The system is relaxed until the root mean square criterion of 0.05 eV/Å on the atomic forces is reached.

The formation energy of a given system is determined using total energy calculations, according to the equation

$$E_f[X] = E_t[X] - n_{Si}\mu_{Si} - n_C\mu_C, \tag{1}$$

where $E_f[X]$ and $E_t[X]$ are the formation and total energies, respectively, of the system X. n_{Si} (n_C) and μ_{Si} (μ_C) represent the number and the chemical potential of the Si (C) atoms present in the system X, respectively. At equilibrium conditions, the net rate of exchange of particles between the SiCNT and the external Si and C atomic sources vanishes. This condition can be expressed as

$$\mu_C + \mu_{Si} = \mu_{SiC}^{tube}. \tag{2}$$

Equation (2) defines a range for the allowable values of the Si and C atomic chemical potentials, with a constraint imposed on their sum. Once the sources are known, atomic chemical potentials can be theoretically determined through total energy calculations. In this work, the Si and C chemical potentials are calculated as the total energy per atom of the most stable bulk configuration, the zinc-blende and the graphite structures, respectively.

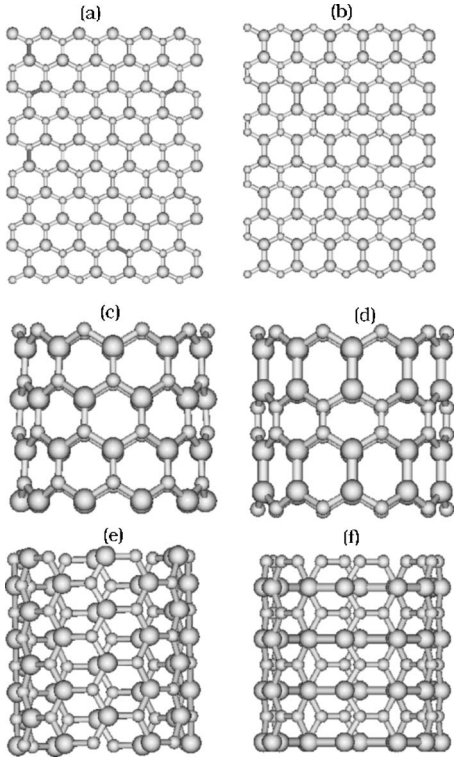

FIG. 1. Type-1 (a), (c), and (e) and type-2 (b), (d), and (f) structures for SiC graphene sheets and tubes (armchair and zigzag). Type-1 structures present only alternating Si-C bonds while in type 2 each Si (C) atom has two C (Si) and one Si (C) atoms as nearest neighbors. The smaller balls represent C atoms while the bigger ones represent Si atoms.

The Si-rich condition can be attained when the nanotube is assumed to be in equilibrium with the Si bulk. In this case we will have $\mu_{Si} \rightarrow \mu_{Si}^{bulk}$, and the C chemical potential (μ_C) is given by Eq. (2); while for the C-rich limit we have $\mu_C \rightarrow \mu_C^{bulk}$, and Eq. (2) defines the remaining chemical potential μ_{Si}. The chemical potential for SiCNT, μ_{SiC}^{tube}, is obtained as the total energy per SiC atomic pairs in the nanotube.

III. RESULTS AND DISCUSSION

Aiming to verify the accuracy of the employed theoretical methodology, initially we performed total energy studies of SiC graphene sheets and nanotubes, and our results were compared with previous (*ab initio*) calculations.[28–30] Two different atomic arrangements for SiC graphene sheets have been considered, viz., (1) alternating Si and C atoms, where each Si (C) atom has only C (Si) atoms as nearest neighbors [Fig. 1(a)], and (2) where the nearest neighbors of each Si (C) atom are two C (Si) atoms and one Si (C) atom, giving rise to Si-Si (C-C) dimers [Fig. 1(b)], type-1 and type-2 graphene sheets, respectively, following the nomenclature proposed by Menon *et al.*[28] Both structural models have a 1:1 Si to C ratio.

We find that the type-1 graphene sheet is energetically more stable than the type-2 graphene sheet by 0.81 eV per Si-C pair. The SiCNTs obtained by rolling up the type-1 graphene sheet [Figs. 1(c) and 1(e)] are energetically more stable by ~0.6 eV per Si-C pair than the ones obtained from the type-2 graphene sheet [Figs. 1(d) and 1(f)]. At the equilibrium geometry, for the SiCNTs formed by type-1 graphene sheets, we find a rippled NT surface, where the more (less) electronegative C (Si) atoms form the outer (inner) shell. A similar equilibrium geometry, i.e., ruled by the electronegativity of the elements, has been observed for BN nanotubes.[39] The energetic preference for the type-1 atomic configuration for both SiC graphene sheets and SiCNTs are in accordance with recent theoretical study performed by Menon *et al.*[28] However, in Ref. 28, using a cluster approach, the authors verified that the armchair (6,6) SiCNT is slightly more stable than the zigzag (12,0) SiCNT, whereas within our large unit cell calculations we do not find any significant energy difference between zigzag (10,0) and armchair (6,6) SiCNTs. Further total energy calculations indicate that the cohesive energy of type-1 SiCNTs (−14.62 eV/Si-C pair) is 1.60 eV higher than the 3*C*-SiC bulk phase. By using a similar calculation approach, Zhao *et al.* obtained a cohesive energy of −15.08 eV per Si-C pair for a (5,5) SiCNT, which is 1.37 eV higher than the one calculated for the 3*C*-SiC bulk phase.[30] At the equilibrium geometry, the Si-C bond distance is around 1.79 Å, depending whether it is perpendicular to or makes a chiral angle with the direction of the tube axis. It is smaller than the Si-C bond length in the 3*C* bulk phase, 1.88 Å. The calculated heat of formation for the SiCNTs is around 1.23 eV, while for the 3*C*-SiC bulk it is −0.36 eV, thus indicating that SiCNTs are metastable structures.

Finally, we examined the electronic band structure for (10,0), (8,4), and (6,6) SiCNTs. The SiCNTs exhibit a semiconducting character, with energy gaps of 1.55, 1.78, and 2.00 eV, for the (10,0), (8,4), and (6,6) SiCNTs, respectively. We verified that the top of the valence band is localized on the carbon atoms, while the bottom of the conduction band lies on silicon, in agreement with previous theoretical calculations.[28–31] Having verified the adequacy of our calculation procedure, we started our study of native defects in SiCNTs.

A. Antisite defects

Antisite defects can be present in semiconducting compounds like SiC. In nanosystems like nanotubes the probability of finding this kind of defect increases because they are grown far from thermodynamic equilibrium. Due to the difference in electronegativity between Si and C atoms, the electronic structure of native defects in SiCNTs should present similarities with their counterparts in III-V nanotubes, with Si and C atoms acting in part as cations and anions, respectively. Antisites in BN nanotubes were theoretically studied[40] and their main characteristics are (i) lower formation energies than the corresponding defects in the BN bulk phase and (ii) introduction of electronic levels within the band gap region. In SiCNTs we can have Si_C, a silicon atom occupying a carbon site, as well as C_{Si}, a carbon atom occupying a silicon site. Our calculated formation energies for Si_C and C_{Si} are summarized in Table I.

TABLE I. Formation energies for antisite defects in SiCNTs.

Defect	Tube chirality	Formation energy (eV)	
		Si rich	C rich
Si_C	Zigzag	2.084	−0.380
C_{Si}	Zigzag	0.354	2.819
Si_C	Armchair	2.129	−0.335
C_{Si}	Armchair	0.335	2.800
Si_C	Mixed	2.098	−0.367
C_{Si}	Mixed	0.261	2.725

Among all the studied defects the Si_C has the lowest formation energy, around −0.38 eV under C-rich conditions, while C_{Si} exhibits formation energy around 0.35 eV at the Si-rich condition. These results are in contrast with the ones obtained for the 3*C*-SiC bulk, viz., we find formation energies of 3.43 and 2.71 eV for Si_C (Si-rich conditions) and C_{Si} (C-rich conditions), respectively. Similar to the ones obtained by Torpo *et al.*[41] (3.1 and 2.83 eV) and by Bernardini *et al.*[42] (3.66 and 2.83 eV), for Si_C (Si-rich conditions) and C_{Si} (C-rich conditions), respectively. Since in single-wall SiCNTs the Si and C atoms are surfacelike, a more effective strain relief process takes place around the antisite atom [see Fig. 2(a) for Si_C in the zigzag (10,0) SiCNT], supporting the lowest formation energies of such defects in SiCNTs. In particular, for Si_C, the local equilibrium geometry shows that the defective atom suffers an outward relaxation, giving rise to a bump of 1.30–1.34 Å (depending on the tube chirality) on the nanotube surface. This bump is due to the greater covalent radius of Si (1.17 Å), as compared to C (0.77 Å), which promotes an sp^3-like hybridization of the Si_C atom. The Si-Si distances of around 2.28 Å are close to the equilibrium distance in the Si bulk. On the other hand, the equilibrium geometry of SiCNT is only slightly perturbed due to the formation of the C_{Si} defect [see Fig. 2(b) for C_{Si} in the zigzag (10,0) SiCNT]. There is no significant radial relaxation, with the C atom not moving outward or inward from the tube surface. The small covalent radius of the substitutional carbon atom leads the first C neighbors to relax, resulting in C-C distances around 1.49 Å, which is an intermediate value between C-C bond distances in diamond and in graphite.

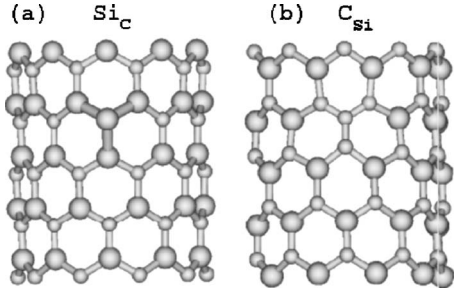

FIG. 2. Geometric structures for the Si_C (a) and C_{Si} (b) defects in a (10,0) zigzag SiC nanotube. The smaller balls represent C atoms and the bigger ones the Si atoms.

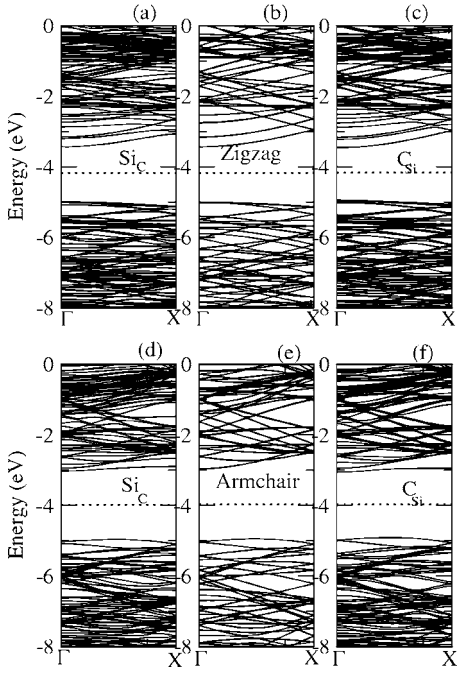

FIG. 3. Band structures for the (10,0) zigzag (a)–(c) and (6,6) armchair (d)–(f) SiCNTs, respectively. Parts (a) and (d) refer to the Si_C defect while parts (c) and (f) are related to C_{Si}. Parts (b) and (e) show the band structures for the perfect zigzag and armchair tubes, respectively. The dotted lines represent the calculated Fermi energy.

The formation energy results for the antisites are consistent with the already stated metastable nature of SiCNTs. It is energetically preferable to arrange the excess Si (C) atoms, at Si-rich (C-rich) conditions, in bulklike phases instead to incorporate the Si (C) atoms at C (Si) sites in the perfect SiCNT. In particular, at C-rich conditions the Si_C formation results an exothermic process. However, the local structure of the nanotube at the Si_C is, as already specified, significantly affected, with the resulting configuration at the antisite position resembling that found in the Si bulk. The tendency in C-rich conditions is clustering of Si atoms at close positions in the nanotube SiCNT, leading to the destabilization of the tubular structure in favor of more compact bulklike structures. This is in agreement with previous theoretical results that predict no tube structures for Si:C ratios greater than 1.[27]

Figures 3(a) and 3(d) present the electronic band structures of Si_C antisites on zigzag (10,0) and armchair (6,6) SiCNTs, respectively. Comparing with the band structure of the defect-free SiCNTs [Figs. 3(b) and 3(e)], we find that this defect, similarly to the case of Si doping in C nanotubes,[43] introduces an empty level within the energy band gap, close and almost parallel to the edge of the conduction band.[44] The highest occupied levels for both chiralities are slightly modified by the presence of antisite defects. For zigzag SiCNTs the empty state (due to the Si_C antisite) exhibits an energy dispersion of around 0.4 eV along the Γ-*X* direction, while the empty state in armchair SiCNTs is almost flat, with an energy dispersion smaller than 0.1 eV. Similarly to the Si_C case, the C_{Si} defect introduces an unoccupied electronic level close to the edge of the conduction band, as shown in Figs. 3(c) and 3(f), for the zigzag and the armchair SiCNTs, respectively. Again, the defective state exhibits a small energy dispersion along the zigzag SiCNT, whereas for the armchair nanotube the defective state is flat along the Γ-*X* direction. The large energy dispersion observed for both antisite defects on (10,0) zigzag nanotube may be related to the well-known underestimation of the energy gap within the LDA approach. That is, such underestimation can gives rise to a somewhat artificial mixing between the (antisite) defect state and conduction bands of SiCNT. Similar artificial mixing was observed by Gali[45] in his LDA calculations for a nitrogen impurity in the carbon site (N_C) in an (8,0) zigzag SiCNT, which was removed by using the BLYP functional to correct the band gap.

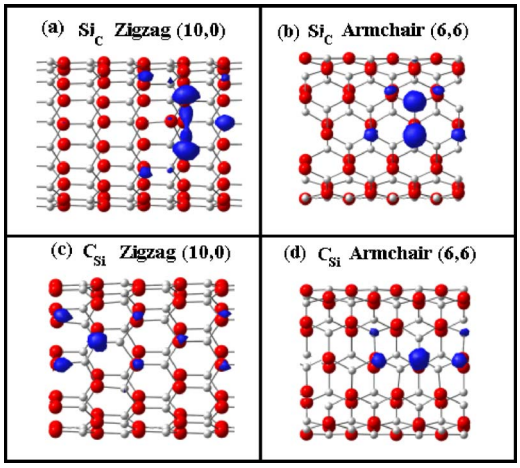

FIG. 4. (Color online) The spatial localization of the lowest unoccupied molecular orbital (LUMO) for the antisite defects in the zigzag [(a) and (b)] and the armchair [(c) and (d)] nanotubes. The smaller (gray) balls represent the C atoms while the bigger ones (red) represent the Si atoms.

Figure 4 presents the charge densities of the empty states introduced by Si_C [Figs. 4(a) and 4(b)] and C_{Si} [Figs. 4(c) and 4(d)] defects in the (10,0) zigzag and (6,6) armchair SiCNTs, respectively. It is noticeable that, for Si_C, the charge density is localized along the Si-Si bonds perpendicular to the tube axis. For C_{Si}, the charge density is localized on the C_{Si} atom, with a small charge density contribution from the second neighboring shell of Si atoms. Furthermore, we observe that for the armchair case [Figs. 4(c) and 4(d)] the charge density is more localized around the defect region, while for the zigzag it is less localized around the antisite atom [Figs. 4(a) and 4(b)], thus supporting the energy dispersion observed in the band structure. The charge densities of the silicon atoms in the Si_C defect indicate a preference for a bonding character, similar to those found in vacancies, which will be discussed at next subsection.

B. Vacancy defects

Vacancies are very important native defects commonly found in semiconducting materials. For carbon and BN nanotubes, the electronic and structural properties induced by the presence of vacancies have been investigated in detail.[40,46] In both cases local bond reconstructions occur, changing the

TABLE II. Formation energies of vacancy defects in SiCNTs.

Defect	Tube chirality	Formation energy (eV)	
		Si rich	C rich
V_C	Zigzag	3.176	1.944
V_{Si}	Zigzag	5.368	6.600
V_C	Armchair	3.496	2.264
V_{Si}	Armchair	6.082	7.314
V_C	Mixed	3.237	2.005
V_{Si}	Mixed	6.855	8.087

original hexagonal network, with the final geometry presenting fivefold and ninefold rings, a defect configuration known in the literature as 51DB.

For carbon nanotubes the main electronic characteristic of a vacancy defect is the appearance of an empty level in the band gap, with the structural reconstructions being verified to be dependent on the nanotube chirality. In BN nanotubes, the boron (V_B) and nitrogen (V_N) vacancies introduce occupied and empty defect levels, respectively, in the band gap region.

In Table II we present the calculated formation energies for single vacancies in SiC nanotubes for both Si- and C-rich conditions. We find that the formation energies of carbon vacancies (V_C) are lower compared with the silicon vacancies (V_{Si}), even under C-rich condition. In addition, the formation energies of vacancies in SiCNTs are lower than their counterparts in the SiC bulk phase.[42,47,48] Indeed, Zywietz *et al.*[47] obtained 4.30 and 8.45 eV for V_C and V_{Si}, respectively, in the (C-rich) 3*C*-SiC bulk. For the three studied SiCNTs, the vacancy reconstructions follow the 51DB pattern [see Fig. 5(a) for V_C in the (10,0) SiCNT]. The Si-Si bond length depends weakly on the tube chirality, being 2.32 Å for the zigzag and 2.37 Å for both armchair and mixed nanotubes. Thus, based upon our total energy results, we can infer that the probability of intrinsic defects (antisites and vacancies) is higher (i.e., they exhibit lower formation energies) in SiCNTs than in the SiC bulk phase.

V_C introduces two defect levels in the gap region [Fig. 6(a)], an occupied level close to the top of the valence band and an empty level close to the bottom of the conduction

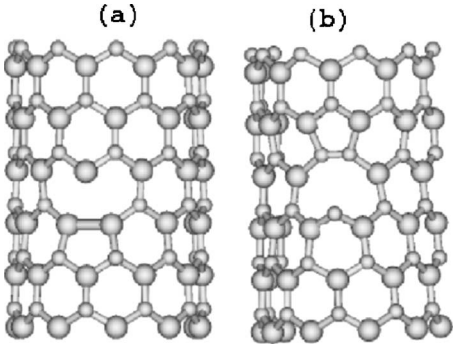

FIG. 5. Geometric structures for the V_C (a) and V_{Si} (b) defects in the (10,0) zigzag SiC nanotube. The smaller balls represent C atoms while the bigger ones represent the Si atoms.

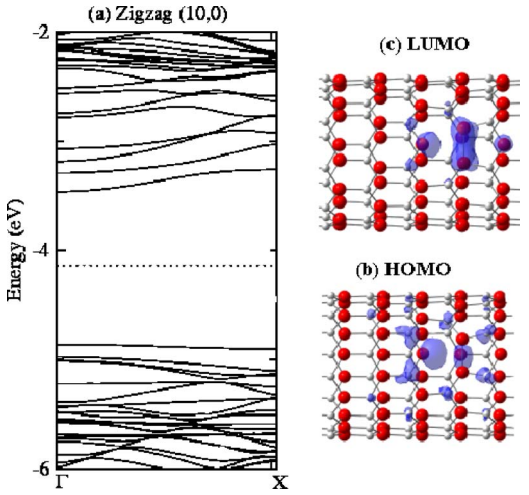

FIG. 6. (Color online) Band structure (a) and spatial charge localization for the occupied (b) and empty (c) levels in the gap region for a carbon vacancy in a zigzag SiCNT. The dotted lines in (a) indicate the Fermi energy. The smaller (gray) balls represent C atoms while the bigger ones (red) represent the Si atoms.

band. These levels are localized on the tube defective region, mainly on the twofold-coordinated Si atom. The charge densities of the occupied and empty levels within the energy gap are shown in Figs. 6(b) and 6(c), respectively. The occupied state is a bonding state, with the charge density lying along the Si-Si dimer, whereas the empty state exhibits an antibonding character, with no charge density along the Si-Si dimer. Similar results were obtained for V_C in armchair (6,6) and mixed (8,4) SiCNTs. It is worth pointing out that, within our spin-polarized calculations, we do not find any spin effect for V_C in SiCNTs.

As indicated in Table II, the formation energies for silicon vacancies (V_{Si}) are the highest ones among the studied intrinsic defects. When a Si is removed from the SiCNT surface, a dangling bond appears for each of the three C atoms in the first neighboring shell. Two of these C atoms move to form a new C-C bond with a local bond reconstruction similar to that observed in CNTs.[46] The third atom remains with a dangling bond, giving rise to the 51DB configuration, as indicated in Fig. 5(b) for V_{Si} in the (10,0) zigzag SiCNT. The reconstructed C-C bond length exhibits a weak dependence on the tube chirality.

Although energetically less favorable, silicon vacancies in SiCNTs present quite interesting electronic properties. The spin-polarized electronic band structures for the V_{Si} are shown in Fig. 7, for zigzag [Figs. 7(a) and 7(b)] and armchair [Figs. 7(c) and 7(d)] SiCNTs. The results for the mixed SiCNT follow closely those obtained for armchair SiCNTs. For both zigzag and armchair systems we find three distinct levels within the band gap, one for the spin-up [Figs. 7(a) and 7(c)] and two for the spin-down [Figs. 7(b) and 7(d)] band structures. The missing (counterpart) spin-up level is resonant within the valence band. The electronic levels within the gap are mainly localized on the three carbon atoms in the first neighboring shell of the vacancy site (see Fig. 8). The spin density is mainly localized on the dangling bond of the twofold-coordinated atom [Figs. 8(a) and 8(d)]

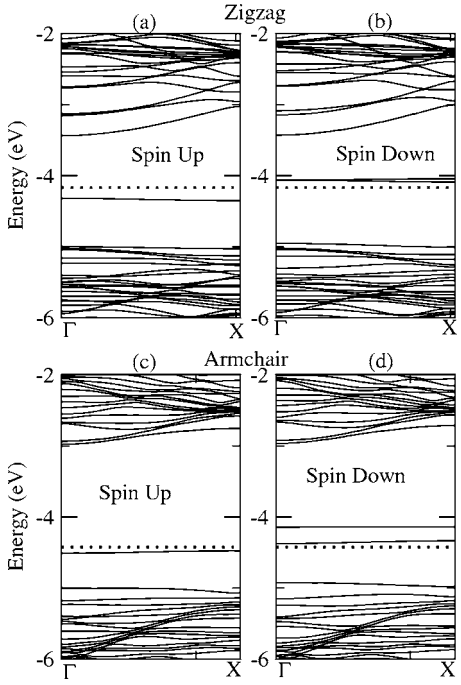

FIG. 7. Band structure for V_{Si} in SiCNTs. Parts (a) and (b) show the results for the zigzag (10,0) nanotube while parts (c) and (d) present the results obtained for the armchair (6,6) nanotube. The dotted lines indicate the Fermi energy.

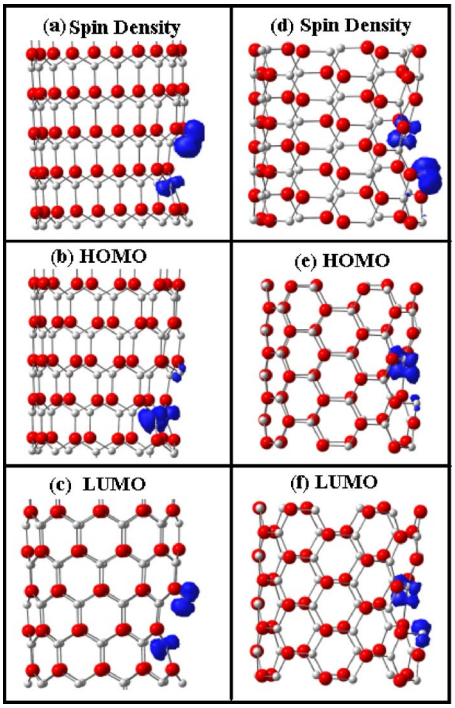

FIG. 8. (Color online) Spin density and charge density localization of the highest occupied (HOMO) and lowest unoccupied molecular orbital (LUMO) levels near the Fermi energy. Parts (a)–(c) show the results for the zigzag (10,0) nanotube and parts (d)–(f) are the results obtained for the armchair (6,6) nanotube. The smaller (gray) balls represent C atoms while the bigger (red) represent the Si atoms.

for the zigzag and armchair SiCNTs, respectively. Similar electronic spin density distribution has been observed for CNTs.[51] The electronic band structures for V_{Si} in SiCNTs, depicted in Fig. 7, reveal a spin-polarized ground state ($S=1$), with an occupied spin-up and two empty spin-down levels within the band gap.

It is worth noting that, due to the fact that the three levels within the band gap are very close in energy, the self-consistent calculations for V_{Si} have been performed using an electronic temperature equal to zero.

The electronic band structures presented in Fig. 7 indicate that the spin-up levels are close to the calculated Fermi energy, and the energy splitting between the two spin-down levels depends on the tube chirality, being greater (smaller) for armchair and chiral (zigzag) SiCNTs nanotubes. It should be noted that the studied nanotubes have different diameters. In order to verify whether the energetic position for these three levels in the gap are diameter dependent, we performed additional calculations for the zigzag nanotubes with greater (11,0) and smaller (9,0) diameters. No such evidence of diameter dependency has been found.

Besides the structural differences between the bulk and the nanotube SiC phases, it is interesting to compare the electronic and spin properties of vacancies for these two phases. A recent *ab initio* study, within the DFT LSDA approach, indicates $S=1$ and $S=0$ total spin states for V_{Si} and V_C, respectively, in SiC bulk.[47] The singlet state of V_C results from a D_{2d} structural distortion of Si neighbors, forming Si dimers. Meanwhile, the same $T_d \rightarrow D_{2d}$ distortion has not been verified for V_{Si}, i.e., the tetrahedral symmetry has been kept, due to the very localized character of C dangling bonds. The resulting states show a (fully occupied) a_1 state and a partially occupied (threefold) degenerate t_2 state, giving rise to a total spin $S=1$ (according to Hund's rule). Subsequent theoretical studies pointed out that the "energy differences between different t_2^α orbital multiplets of the same spin state" cannot be accurately obtained within the DFT LSDA approach.[49] By using self-consistent multiconfigurational (MC) calculations for saturated SiC clusters Deak *et al.*[49] obtained a singlet state for V_{Si}. This result was confirmed by recent *ab initio* studies within the supercell approach.[50] Since for silicon vacancy in SiCNTs the two empty spin-down and the spin-up states near the Fermi energy are quite close in energy, there is a possibility that MC calculations could lead to a singlet ground state. We believe that further investigation, including MC calculations, is necessary to clarify this issue.

The charge densities of the electronic states (occupied and empty) within energy band gap for V_{Si} in zigzag and armchair SiCNTs are depicted in Figs. 8(b), 8(c), 8(e), and 8(f), respectively. We can verify that the occupied level presents greater contributions from the threefold coordinated C atoms while the empty level comes from the twofold-coordinated C atom near the V_{Si} site. The charge density of the other spin-down level in the gap (LUMO+1), which remains empty for all the studied cases, shows main contributions of the p level of the twofold-coordinated C atom. It is interesting to observe that the spin-up level in the zigzag nanotube shares the mirror symmetry of the zigzag nanotube. For the other nanotube configurations this symmetry is completely lost. The

bonding distance of this reconstructed C-C bond is 1.44 Å for the zigzag, 1.46 Å for the armchair, and 1.47 Å for the mixed case. Thus, the orientation of the reconstructed C-C bond in the nanotubes can be crucial to determine the energetic position of the levels within the nanotube gap.

The use of a nonzero electronic temperature (during the self-consistent procedure) promotes a partial occupation of the almost degenerate levels within the nanotube gap. It can indeed change the total spin state of the system. By increasing the electronic temperature, the electrons will be promoted from the spin-up to the spin-down levels, decreasing (increasing) the exchange interactions between the spin-up (spin-down) levels and leading to possible reordering of these levels. The calculated band structures obtained with a 0 K electronic temperature (Fig. 7), show that it should be much more pronounced for the armchair and the mixed tubes than for the zigzag tube because the energy difference between the spin-up level (occupied) and the lowest one of the spin-down levels is greater for the zigzag than for the others.

IV. CONCLUSIONS

Using local spin density functional calculations we studied the energetic, stability, equilibrium geometries, and electronic properties of neutral native defects in SiC nanotubes, viz., antisites (Si_C and C_{Si}) and vacancies (V_{Si} and V_C). We find that Si_C defects, under C-rich conditions, exhibit the lowest formation energies, around −0.38 eV, followed by C_{Si} (formation energies of ~0.35 eV at Si-rich conditions). The main electronic feature of these defects is an empty electronic level close to the bottom of the conduction band, keeping the semiconducting character of SiC nanotubes. Vacancies present higher formation energies, with V_{Si} being the energetically less favorable defect (formation energy higher than 5 eV). For the carbon vacancy V_C two levels appear in the energy band gap, one occupied (bonding) near the valence band maximum, and the other empty (antibonding) close to the conduction band minimum. The characteristic features of V_{Si} are a spin-up level resonant within valence band and three almost degenerate levels (one for spin up and two for spin down) within the nanotube gap. The energetic ordering of these three levels can induce a $S=1$ total spin state, with the net spin density localized on the defective region (twofold-coordinated C atom with a dangling bond). However, we believe that further calculations are necessary to support (or not) this finding for the ground state of V_{Si} in SiCNTs.

ACKNOWLEDGMENTS

All calculations were performed using the computational facilities of the Centro Nacional de Processamento de Alto Desempenho/CENAPAD-Campinas. This work has been supported by the Brazilian agencies CNPq, FAPEMIG, and FAPERGS.

*Electronic address: rbaierle@smail.ufsm.br

[1] S. Iijima, Nature (London) **354**, 56 (1991).
[2] R. Saito, G. Dresselhaus, and M. S. Dresselhaus, *Physical Properties of Carbon Nanotubes* (World Scientific, London, 1998).
[3] R. Saito, M. Fujita, G. Dresselhaus, and M. S. Dresselhaus, Appl. Phys. Lett. **60**, 2204 (1992).
[4] S. J. Tans, M. H. Devoret, H. Daí, A. Thess, R. E. Smalley, L. J. Geerligs, and C. Dekker, Nature (London) **386**, 474 (1997).
[5] S. M. Lee, Y. H. Lee, Y. G. Hwang, J. Elsner, D. Porezag, and T. Frauenheim, Phys. Rev. B **60**, 7788 (1999).
[6] G. Seifert and E. Hernandez, Chem. Phys. Lett. **318**, 355 (2000).
[7] Y. R. Hacohen, E. Grunbaum, R. Tenne, and J. L. Hutchison, Nature (London) **395**, 336 (1998).
[8] Y. Feldman, E. Wasserman, D. J. Srolovitz, and R. Tenne, Science **267**, 222 (1995).
[9] C. Balasubramanian, S. Belluci, P. Castrucci, M. De Crescenzi, and S. V. Bhoraskar, Chem. Phys. Lett. **383**, 188 (2004).
[10] L. Bourgeois, Y. Bando, W. Q. Han, and T. Sato, Phys. Rev. B **61**, 7686 (2000).
[11] Y. Cui and C. M. Lieber, Science **291**, 851 (2001).
[12] S. B. Fagan, R. J. Baierle, R. Mota, A. J. R. da Silva, and A. Fazzio, Phys. Rev. B **61**, 9994 (2000).
[13] G. Seifert, Th. Kohler, K. H. Urbassek, E. Hernández, and T. Frauenheim, Phys. Rev. B **63**, 193409 (2001); G. Seifert, Th. Kohler, Z. Hajnal, and T. Frauenheim, Solid State Commun. **119**, 653 (2001).
[14] Y. Ryu, Y. Tak, and K. Yong, Nanotechnology **16**, S370 (2005).
[15] G. Xi, Y. Peng, S. Wan, T. Li, W. Yu, and Y. Qian, J. Phys. Chem. B **108**, 20102 (2004).
[16] A. P. Alivisatos, Science **271**, 933 (1996).
[17] E. W. Wong, P. E. Sheehan, and C. M. Lieber, Science **277**, 1971 (1997).
[18] Ruoxi Wang, Dongju Zhang, and Chengbu Liu, Chem. Phys. Lett. **411**, 333 (2005).
[19] *Properties of Silicon Carbide*, edited by G. L. Harris (INSPEC, Institution of Electrical Engineers, London, 1995).
[20] Z. Pan, H.-L. Lai, F. C. K. Au, X. Duan, W. Zhou, W. Shi, N. Wang, C-S. Lee, N.-B. Wong, S.-T. Lee, and S. Xie, Adv. Mater. (Weinheim, Ger.) **12**, 1186 (2000).
[21] Z. C. Feng, A. J. Mascarenhas, W. J. Choyke, and J. A. Powell, J. Appl. Phys. **64**, 3176 (1998).
[22] Cuong Pham-Huu, Nicolas Keller, Gaby Ehret, and Marc J. Ledoux, J. Catal. **200**, 400 (2001).
[23] X.-H. Sun, C.-P. Li, W.-K. Wong, N.-B. Wong, C.-S. Lee, S.-T. Lee, and B.-K. Teo, J. Am. Chem. Soc. **124**, 14464 (2002).
[24] J. Q. Hu, Y. Bando, J. H. Zhan, and D. Golberg, Appl. Phys. Lett. **85**, 2932 (2004).
[25] Hao Wang, Xiao-Dong Li, Taek-Soo Kim, and Dong-Pyo Kim, Appl. Phys. Lett. **86**, 173104 (2005).
[26] E. Borowiak-Palen, M. H. Ruemmeli, T. Gemming, M. Knupfer, K. Biedermann, A. Leonhart, T. Pichler, and R. J. Kalenczuk, J. Appl. Phys. **97**, 056102 (2005).
[27] A. Mavrandonakis, G. E. Froudakis, M. Schnell, and M. Muhlhauser, Nano Lett. **3**, 1481 (2004).

[28] M. Menon, E. Richter, A. Mavrandonakis, G. Froudakis, and A. N. Andriotis, Phys. Rev. B **69**, 115322 (2004).
[29] Y. Miyamoto and B. D. Yu, Appl. Phys. Lett. **80**, 586 (2002).
[30] Mingwen Zhao, Yueyuan Xia, Feng Li, R. Q. Zhang, and S.-T. Lee, Phys. Rev. B **71**, 085312 (2005).
[31] Mingwen Zhao, Yueyuan Xia, R. Q. Zhang, and S-T. Lee, J. Chem. Phys. **112**, 214707 (2005).
[32] D. M. Ceperley and B. J. Alder, Phys. Rev. Lett. **45**, 566 (1980).
[33] J. P. Perdew and A. Zunger, Phys. Rev. B **23**, 5048 (1981).
[34] P. Ordejón, E. Artacho, and J. M. Soler, Phys. Rev. B **53**, R10441 (1996); D. Sanchez-Portal, P. Ordejón, E. Artacho, and J. M. Soler, Int. J. Quantum Chem. **65**, 453 (1997).
[35] O. F. Sankey and D. J. Niklewski, Phys. Rev. B **40**, 3979 (1989).
[36] N. Troullier and J. L. Martins, Phys. Rev. B **43**, 1993 (1991).
[37] L. Kleinman and D. M. Bylander, Phys. Rev. Lett. **48**, 1425 (1982).
[38] H. J. Monkhorst and J. D. Pack, Phys. Rev. B **13**, 5188 (1976).
[39] D. Goldberg, Y. Bando, L. Bourgeois, K. Kurashima, and T. Sato, Appl. Phys. Lett. **77**, 1979 (2000).
[40] T. M. Schmidt, R. J. Baierle, P. Piquini, and A. Fazzio, Phys. Rev. B **67**, 113407 (2003); P. Piquini, R. J. Baierle, T. M. Schmidt, and A. Fazzio, Nanotechnology **16**, 827 (2005).
[41] L. Torpo, S. Pöykkö, and R. M. Nieminen, Phys. Rev. B **57**, 6243 (1998).
[42] F. Bernardini, A. Mattoni, and L. Colombo, Eur. Phys. J. B **38**, 437 (2004).
[43] R. J. Baierle, S. B. Fagan, R. Mota, A. J. R. da Silva, and A. Fazzio, Phys. Rev. B **64**, 085413 (2001).
[44] Even thought the DFT LDA is well known to understimate the gap energy, it provides reliable results for the trend in the position of the levels in the gap; see, for example, A. Fazzio, A. Janotti, A. J. R. da Silva, and R. Mota, Phys. Rev. B **61**, R2401 (2000); M. J. Puska, S. Poykko, M. Pesola, and R. M. Nieminen, *ibid.* **58**, 1318 (1998).
[45] A. Gali, Phys. Rev. B **73**, 245415 (2006).
[46] J. Rossato, R. J. Baierle, A. Fazzio, and R. Mota, Nano Lett. **5**, 197 (2005).
[47] A. Zywietz, J. Furthmüller, and F. Bechstedt, Phys. Rev. B **59**, 15166 (1999).
[48] C. Wang, J. Bernholc, and R. F. Davis, Phys. Rev. B **38**, 12752 (1998).
[49] P. Deák, J. Miró, A. Gali, L. Udvardi, and H. Overhof, Appl. Phys. Lett. **75**, 2103 (1999).
[50] A. Zywietz, J. Furthmüller, and F. Bechstedt, Phys. Rev. B **62**, 6854 (2000).
[51] Y. Ma, P. O. Lehtinen, A. S. Foster and R. M. Nieminen, New J. Phys. **6**, 68 (2004); Y. Ma, P. O. Lehtinen, A. S. Foster, and R. M. Nieminen, Phys. Rev. B **72**, 085451 (2005).